WL-EMP-IN-113

INTERACTION NOTES

NOTE 113

7 June 1972

THE EXTENDED BOUNDARY CONDITION SOLUTION OF THE DIPOLE ANTENNA OF REVOLUTION

Clayborne D. Taylor
Mississippi State University
State College, Mississippi 39762

Donald R. Wilton
The University of Mississippi
University, Mississippi 38677

dipoles antennas, bodies of revolution

ABSTRACT

Applying Waterman's extended boundary condition a general formulation is developed for the dipole antenna of revolution. Both transmission and scattering from the antenna are considered with no formal restrictions on the antenna dimensions. As examples the prolate spheroidal and solid cylindrical geometries are considered.

PROLEGOMENA

Often it is necessary to know the induced surface currents and charges on shielded configurations in order to assess the shielded integrity. In developing a tractable analysis for obtaining the surface currents and charges one is usually forced to make gross approximations to the physical configuration of the shield. For example a box is represented by a sphere, a missile is represented by a right circular cylinder and an aircraft is represented by perpendicular crossed cylinders. This paper presents an attempt at analyzing a class of somewhat more complex structures than have been considered previously in approximating shield configurations. Furthermore the analysis of these structures, bodies of revolution, is no more complicated.

Perhaps the most important advantage of the presented formulation is the capability of being extended to structures formed from segments of bodies of revolution. For example, in the analysis of EMP interaction with an aircraft, the aircraft may be represented by sections of bodies of revolution. This analysis is to appear in the near future as an interaction note.

INTRODUCTION

In the conventional formulation of the dipole antenna problem an integral equation for the antenna current distribution is derived by forcing the component of the scattered electric field tangential to the antenna surface to cancel the corresponding component of the incident field over the antenna surface. In so doing the integral equation is obtained with a kernel that has a logarithmic singularity.[1*]

*The superscripts refer to the list of references at the end of the paper.

TABLE 2: MONOPOLE ADMITTANCE FOR FLAT END CAP

$a/\lambda = 0.0423$, $b/a = 1.187$

h/λ	$Y^*_{measured}$	Y_{TEM}	N
0.12	5.6 + i 26.9 m℧	6.11 + i 27.15 m℧	14
.16	19.8 + i 30.6	20.42 + i 30.30	14
.20	29.8 + i 12.8	30.82 + i 12.29	14
.24	19.6 + i 3.7	20.75 + i 2.04	14
.28	12.9 + i 3.9	13.67 + i 2.03	14
.32	9.5 + i 5.7	9.78 + i 5.16	34
.36	7.6 + i 7.7	7.91 + i 6.92	34
.40	6.6 + i 9.6	6.81 + i 8.58	34
.44	6.0 + i 11.5	6.16 + i 10.21	34
.48	5.7 + i 13.4	5.87 + i 11.94	34
.52	5.9 + i 15.4	5.98 + i 13.91	34
.56	6.8 + i 18.0	6.83 + i 16.33	34
.60	9.3 + i 21.8	9.34 + i 19.18	34
.64	15.4 + i 22.3	15.54 + i 20.98	44
.68	21.7 + i 16.4	22.23 + i 14.78	44
.72	18.7 + i 8.5	19.56 + i 6.54	44

*Measured by S. Holly[12]

discontinuities do occur, such as for a solid cylinder with flat end faces, an approximate technique is used that in general is quite accurate for relatively thin antennas, i.e. for $a/\lambda < .1$ where a is the antenna radius. The current distribution on the discontinuity is obtained from a quasi-static approximation.

To illustrate the use of the presented formulation it is applied to treat the solid cylindrical antenna and the prolate spheroidal antenna. The transmitting current distribution and antenna impedances are obtained for the solid cylindrical antenna. Also the current distributions induced by an incident plane wave illumination are obtained for the prolate spheroid. Comparisons of the theoretical results with experimental data are made.

ANALYSIS

General Considerations

In the presence of a metallic body the total electric field may be expressed in terms of the induced surface current on the body as[4]

$$\vec{E}(\vec{R}) = \vec{E}^{inc}(\vec{R}) - i\frac{\eta}{4\pi k}\left\{\nabla\int_S \nabla' \cdot \vec{J}(\vec{R}')G(\vec{R},\vec{R}')ds' + k^2\int_S \vec{J}(\vec{R}')G(\vec{R},\vec{R}')ds'\right\} \quad (1)$$

where $\vec{E}^{inc}$ is the incident or impressed electric field, $\vec{J}$ is the induced surface current on the metallic surface S, k is the propagation constant, $\eta = \sqrt{\mu_o/\varepsilon_o} \simeq 120\pi$ ohms is the intrinsic wave impedance of free space, $\vec{R}'$ is the radius vector to the differential surface element ds', and

$$G(\vec{R},\vec{R}') = \frac{e^{-ik|\vec{R}-\vec{R}'|}}{|\vec{R}-\vec{R}'|} \tag{2}$$

Consider a body of revolution having its symmetry axis coincident with the z axis of a cylindrical coordinate system (see figure 1). Then

$$ds' = a(z')d\phi'dz'/\cos\theta(z') \tag{3}$$

$$\frac{d}{dz'}\, a(z') = \tan\theta(z') \tag{4}$$

$$|\vec{R}-\vec{R}'| = \sqrt{r^2 + r'^2 - 2rr'\cos(\phi-\phi') + (z-z')^2} \tag{5}$$

$$\nabla'\cdot\vec{J}(\vec{R}') = \frac{1}{a(z')}\left\{\frac{\partial}{\partial\phi'}\, J_{\phi}' + \frac{\partial}{\partial t'}\,[a(z')J_{t'}]\right\} \tag{6}$$

$$\hat{t}' = \hat{z}'\cos\theta(z') + \hat{r}'\sin\theta(z') \tag{7}$$

$$dz' = dt'\cos\theta(z') \tag{8}$$

where (r,ϕ,z) are the usual cylindrical coordinates and θ is defined in fig. 1. Here $\hat{t}'$ is the unit vector tangential to the surface of the body yet perpendicular to $\hat{\phi}$. Ultimately (1) will be evaluated at $r = 0$ and $0 < z < L$, i.e. on the axis of and within the body of revolution. To that end consider the first integral

evaluated at r = 0. It is

$$\int_S \nabla' \cdot \vec{J}(\vec{R}')G(\vec{R},\vec{R}')ds' \Big|_{r=0} = \int_0^L dz' \; K(z,z') \frac{\partial}{\partial z'} [a(z') \cdot \int_{-\pi}^{\pi} d\phi' \; J_t(z',\phi')] \tag{9}$$

where

$$K(z,z') = \exp[-ik\sqrt{(z-z')^2+a^2(z')}]/\sqrt{(z-z')^2+a^2(z')} \tag{10}$$

Now consider the axial component of the second integral of (1) evaluated at r = 0 and 0 < z < L.

$$\hat{z} \cdot \int_S \vec{J}(\vec{R}')G(\vec{R},\vec{R}')ds' = \int_0^L dz' \; \frac{K(z,z')}{\cos\,\theta(z')} [a(z') \int_{-\pi}^{\pi} d\phi' J_z(z',\phi')] \tag{11}$$

Further it is noted

$$J_z(z',\phi') = [\cos\,\theta(z')] J_t'(z',\phi') \tag{12}$$

and

$$I_t'(z') = a(z') \int_{-\pi}^{\pi} d\phi' \; J_t'(z',\phi') \tag{13}$$

is the total current through the cross section at z' along the axis of the body.

To obtain the integral equation for the current distribution the z-component of (1) is evaluated at r = 0 and 0 < z < L using (9) and (11)-(13). This yields

$$E_z(0,\phi,z) = E_z^{inc}(0,\phi,z) - i \frac{\eta}{4\pi k} [\int_0^L dz' \; \frac{\partial}{\partial z'} I_t(z') \frac{\partial}{\partial z} K(z,z') + k^2 \int_0^L dz' \; I_t'(z') \; K(z,z')] \tag{14}$$

On the axis of and within the body of revolution the axial component of the electric field is required to vanish as opposed to the conventional procedure of requiring the tangential component of the electric field to vanish at the surface of the conductor. Then (14) yields after some mathematical manipulation

$$\int_0^L dz' \; I_t'(z')\left(k^2 - \frac{\partial^2}{\partial z \partial z'}\right) K(z,z') + I_t'(z') \frac{\partial}{\partial z} K(z,z') \Bigg|_0^L$$

$$= - i \frac{4\pi k}{\eta} E_z^{inc}(0,\phi,z) \qquad \text{for} \quad 0 < z < L \qquad (15)$$

If the current vanishes at both ends of the body of revolution then (15) takes the form analogous to that derived by Hallén[5] and later by Albert and Synge.[6*] The Hallén integral equation equivalent of (15) is derived in the appendix.

Up to this point the body of revolution is required to have no discontinuities in radius, i.e. a(z) must be differentiable. If the body of revolution has radius discontinuities the integral equation must be modified. This modification consists of two parts: (1) continuity of current must

*Hallén as well as Albert and Synge claim that (15) or their equivalent is exact. Furthermore, Hallén argues that the solution is unique. The accuracy of the numerical results subsequently presented also indicate the uniqueness of solution.

be preserved at the discontinuity and (2) the incident field on the continuous portion of the body is forced to include the scattered field from the discontinuity with an assumed current distribution. To solve the problem rigorously is a formidable task. However, for a surface with characteristic dimensions much less than a wavelength a quasi-static type approximation for the functional form of the current and the use of the aforementioned modifications should yield a suitably accurate current distribution for the body. This is to be the procedure followed in the subsequent analysis.

For the transmitting problem the antenna is considered to be driven from a magnetic current source. The monopole of revolution is connected to the center conductor of a coaxial transmission line which terminates in a ground plane at $z=0$. It may then be treated as a dipole by image theory where the field distribution in the gap of the coaxial line is represented by a magnetic current frill[6,10]. Further considering only the TEM mode existing in the coaxial line the impressed electric field component is[10]

$$E_z^{inc}(0,\phi,z) = \frac{V_o}{2\ell n(b/a)}\left[\frac{e^{-ik\sqrt{(z-z_o)^2+a^2}}}{\sqrt{(z-z_o)^2+a^2}} - \frac{e^{-ik\sqrt{(z-z_o)^2+b^2}}}{\sqrt{(z-z_o)^2+b^2}}\right] \qquad (16)$$

where a and b are the inner and outer radii of the coaxial line. Also a is the radius of the dipole antenna at the driving point $z = z_o$, i.e. $a = a(z_o)$.

For the scattering problem the dipole of revolution is considered to be illuminated by a plane wave. Then

$$E_z^{inc}(0,\phi,z) = E_o \sin\theta_o \, e^{-i(k\cos\theta_o)z} \tag{17}$$

where the direction of propagation forms an angle θ_o with the positive z-axis and E_o is the complex amplitude of the electric field.

Prolate Spheroid

The prolate spheroid is a good example to consider since it is amenable to solution by boundary value problem techniques. The surface of the spheroid is given by

$$a(z) = \left((\varepsilon^{-2} - 1)\,[F^2 - (z-L/2)^2\varepsilon^2]\right)^{\frac{1}{2}} \tag{18}$$

where ε is the eccentricity, 2F is the interfocal distance, and L is the total length of the spheroid measured along the axis of symmetry. In the foregoing the spheroid extends from z = 0 to z = L.

An integral equation for the current distribution is obtained by using (18) in (15) noting that

$$I_t(z)\Big|_{z = 0,L} = 0$$

Solid Cylinder with Flat End Faces

For this configuration the integral equation for the induced current distribution must be modified. The functional form for the current on the end is obtained from a quasi-static type approximation. Accordingly the end face charge distribution is approximated

$$\rho(r) \simeq \frac{Q}{\pi a^2} \tag{19}$$

where a is the radius of the end face and Q the total charge on the end face. Using the equation of continuity and requiring a zero current at the center of the end face yields for the end face current distribution

$$J_r(r) \simeq - \frac{i\omega Q}{2\pi a^2} r \tag{20}$$

Also requiring continuity of current around the edges of the end face yields

$$Q \simeq I_t(o)/(-i\omega) \tag{21}$$

Note that the current distribution given in (20) compares quite favorably with that obtained by Einarson[7] using a numerical solution technique.

The axial component of the electric field scattered from the end face with the assumed current distribution is readily shown to be, after some mathematical manipulation.

$$E_o^c(z) = i \frac{\eta I_t(0)}{2\pi k a^2} z\left[\frac{e^{-ik|z|}}{|z|} - K_a(z,0)\right] \tag{22}$$

where

$$K_a(z,z') = \frac{\exp\left[-ik\sqrt{(z-z')^2 + a^2}\right]}{\sqrt{(z-z')^2 + a^2}} \tag{23}$$

Furthermore, at the opposite end of the cylinder there is another contribution to the axial component of the scattered

electric field.

If the aforementioned scattered fields are considered as contributions to the incident field, (15) yields the following integral equation for the current distribution on a perfectly conducting solid cylinder with flat end caps:

$$\int_0^L dz' \; I_{t'}(z') \; K_{t'}(z,z') = - i \frac{4\pi k}{\eta} E_z^{inc} (0,\phi,z)$$

$$\text{for } 0 < z < L \tag{24}$$

where

$$K_{t'}(z,z') = (k^2 + \frac{\partial^2}{\partial z^2}) K_a(z,z') - 2\delta(z') \frac{\partial}{\partial z} K_a(z,0)$$

$$-2\delta(L-z') \frac{\partial}{\partial z} K_a(z,L) - \frac{4\delta(z')}{a^2} [e^{-ikz} - z \; K_a(z,0)]$$

$$- \frac{4\delta(L-z')}{a^2} [e^{-ik(L-z)} - (L-z) \; K_a(z,L)] \tag{25}$$

and $\delta(z)$ is the Dirac delta.

NUMERICAL RESULTS

The integral equations derived in the foregoing analysis may be solved numerically by using the so called method of moments.[8] It has been shown that the piecewise sinusoidal expansion for the current distribution in the method of moments provides a rapidly convergent solution. According

to this technique the current is

$$I_t'(z') = \sum_{m=1}^{N} I_m(z')\, U(z';\, z_{m+1},\, z_m) \tag{26}$$

where

$$I_m(z') = \frac{\alpha_{m+1} \sin k(z' - z_m) + \alpha_m \sin k(z_{m+1} - z')}{\sin k(z_{m+1} - z_m)} \tag{27}$$

$$U(z';z_{m+1},\, z_m) = 1 \qquad z_m < z' < z_{m+1}$$

$$= 0 \qquad \text{otherwise}$$

with z_m as a convenient ordered set of points on the domain of the current including the end points.

Substituting the current expansion into the integral equation for the current and forcing the resulting equation to be satisfied at a suitable set of points yields a system of linear equations for the expansion coefficients. Also boundary conditions on the current must be satisfied.

Prolate Spheroid

The total axial current induced on a prolate spheroid illuminated by an incident plane wave may be obtained by solving the appropriate boundary value problem.[9] Unfortunately the solution obtained is an infinite series of spheroidal wave functions. Although the series is highly convergent, it may be more practical to use the integral equation formulation presented here. A comparison of the results is given in Table 1. The integral equation solution was obtained by N = 21 in the current expansion (26).

Monopole Antenna with Flat End Faces

Since there is no formal restriction on the size of

antennas which can be treated here, it is desired to test the method for antennas whose circumference is comparable to the wavelength. This then requires consideration of the end face currents as given in equation (24). For an antenna with a constant radius, the second derivative with respect to z in (25) may be replaced by a second derivative with respect to z' because of the difference form of the argument of the kernel in (22). Using (26) in (24) and some mathematical manipulation allows the evaluation of all matrix elements without numerical integration.

Table 2 gives the calculated and measured admittance[12] of a monopole antenna above a ground plane fed by a coaxial line whose outer conductor terminates in the ground plane, the extension of the inner conductor forming the monopole. Here h is the height of the monopole. For the calculated data, equation (16) was used for the excitation, thus ignoring higher order modes in the coaxial aperture. This neglect of the higher order modes may account in part for the differences in the measured and computed data.

In Table 3, the results for a relatively thick monopole antenna are shown. No estimate of the effect of higher order modes on the admittances calculated is available for this case but it is expected that the necessary correction would be considerable. Furthermore, the large radius may lead one to question the validity of the approximation used to account for the end face of the antenna. Nevertheless, good agreement is seen between the calculated and experimental values.

It was found that for thick structures, the smooth nature of the kernel in (24) and in the driving function (16) enable one to get reasonably good convergence with relatively few zones over the antenna. In fact, the use of too many zones caused the system of equations to become very ill-conditioned and to yield meaningless current distribution. It was found that by choosing the numbers of zones so that the normalized determinant[13] of the system always remained above 10^{-4}, reasonable current distributions and admittances were obtained. Increasing the number of zones further caused large oscillations in the currents and very large admittance values. It appears that to insure stability and accuracy one should choose the zones such that the width of a zone is no smaller than about a/4 and no larger than 2a.

Monopole Antenna with Sperical End Cap

When the end cap of a cylindrical antenna possesses no surface discontinuities then (15) may be applied directly. One particularly interesting such end configuration for a cylindrical monopole is the spherical end cap. Actually the end of the cylinder may be considered a hemisphere with radius equal to the radius of the cylindrical monopole. In Table 4 the current distributions on a given antenna is shown for spherical end caps and flat end caps. The measured driving point current for the spherical end cap is also shown. Note that the calculated values agree with the measured result. Further, it is noted that the antenna current, especially the imaginary part, for this relatively thin antenna is almost insensitive to the end configuration.

It is also of interest to consider the thick cylindrical monopole with a spherical end cap. Table 5 exhibits the corresponding measured and calculated admittances. The measured data is obtained from King's tables of antenna characteristics.[12] Although he defines h as the height of the monopole not including the end cap, recently it was determined that h in the King's tables of data for monopole with spherical end cap included the end cap.[14] Excellent agreement is obtained. Note that for $h/\lambda = .12$ the diameter of the monopole is nearly twice the height. Further note that $h = L/2$.

CONCLUSION

A formally exact integral equation has been presented for the dipole antenna of revolution. Solution of the integral equation yields the total axial current even for circumferentially dependent incident fields. Furthermore, the integral equation has a regular kernel and in principle is valid for thick as well as thin antennas. For very thick antennas, convergence to a solution is rapid, but numerical instabilities begin to appear and some caution must be exercised.

For thin and moderately thick antennas, excellent agreement is obtained when theoretical results are compared with experimental data. In the case of scattering from a prolate spheroid an exact boundary value problem solution is available. A comparison of the results from the presented formulation with the boundary value solution yields excellent agreement. Results for the current distribution on a cylinder with flat end faces seem to justify the use of the leading term in a quasi-static approximation for the end face current. Furthermore, the technique can readily be adapted for use with antennas having stepped

radii. However, it is felt that the method may be unsuitable for antennas with radius greater than about 0.1λ.

Finally it is noted that by using the extended boundary condition one is able to evaluate analytically the field contributions due to the end faces and the frill sources. With the conventional solution technique these field contributions must be obtained by numerical integration.[18,19]

ACKNOWLEDGEMENT

The authors wish to thank Mr. Robert F. McKinney for his assistance in the numerical computations and Dr. C. E. Baum for reading the manuscript.

REFERENCES

1. C. W. Harrison, Jr., C. D. Taylor, E. E. O'Donnell and E. A. Aronson, "On Digital Computer Solutions of Fredholm Integral Equations of the First and Second Kind Occurring in Antenna Theory," Radio Science, Vol. 2 (New Series), No. 9, pp. 1067-1081, September 1967.

2. P. C. Waterman, "New Formulation of Acoustic Scattering," J. Acoust. Soc. Amer., Vol. 45, No. 6, pp. 1417-1429, June 1969. (see also P. C. Waterman, Proc. IEEE, Vol. 53, No. 8, pp. 785-812, August 1965).

3. J. H. Richmond, "Digital-Computer Solutions of the Rigorous Equations for Scattering Problems," Proc. IEEE, Vol. 53, No. 8, pp. 796-804, August 1965.

4. D. S. Jones, The Theory of Electromagnetism, (Pergamon Press: New York, 1964) p. 55.

5. E. Hallén, "Theoretical Investigations into the Transmitting and Receiving Qualities of Antennas," Nova Acta Regiae Societatis Scientiarium Upsaliensis, Series IV, Vol. II, No. 4, pp. 1-44, 1938.

6. G. E. Albert and J. L. Synge, "The General Problem of Antenna Radiation and the Fundamental Integral Equation, with Application to an Antenna of Revolution - Part I," Quart. Appl. Math., Vol. 6, pp. 117-131, April 1948, (see also J. L. Synge, Quart. Appl. Math., Vol. 6, pp. 133-156, April 1948).

7. O. Einarsson, "Comparison Between Tube-Shaped and Solid Cylinder Antennas," IEEE Trans. Antennas and Prop., Vol. AP-14, No. 1, pp. 31-37, January, 1966.

8. R. F. Harrington, Field Computation by Moment Methods, (The MacMillan Company: New York, 1968).

9. C. D. Taylor, "On the Exact Theory of a Prolate Spheroidal Receiving and Scattering Antenna, Radio Science, Vol. 2 (new series), No. 3, pp. 351-360, March 1967.

10. L. L. Tsai, "A Numerical Solution for the Near and Far Fields of an Annular Ring of Magnetic Current," IEEE Trans. Ant. Prop., September, 1972.

11. C. Flammer, "The Prolate Spheroidal Monopole Antenna," Standford Research Institute, Tech. Rept. 22, Menlo Park, Calif., 1957.

12. R. W. P. King, Tables of Antenna Characteristics, (IFI/Plenum: New York, 1971) Section 2.

13. Conte, S. D., Elementary Numerical Analysis, McGraw-Hill, New York 1965.

14. R. W. P. King, private communication.

15. S. A. Schelkunoff, Advanced Antenna Theory, New York: Wiley, 1952, p. 132.

16. K. K. Mei, "On the Integral Equation of Thin Wire Antennas," IEEE Trans. Ant. Prop., Vol. AP-13, pp. 374-378, May 1965.

17. G. K. Cambrell and C. T. Carson, "On Mei's Integral Equation of Thin Wire Antennas," IEEE Trans. Ant. Prop., Vol. AP-19, pp. 781-782, November 1971.

18. R. W. Sassman, "The Current Induced on a Finite, Perfectly Conducting, Solid Cylinder in Free Space by an Electromagnetic Pulse," Interaction Note 11, 1967.

19. M. I. Sancer and A. D. Varvatsis, "Calculation of the Induced Current Density on a Perfectly Conducting Body of Revolution," Interaction Note 101, April 1972.

APPENDIX

The integro-differential equation for the current distribution on the body of revolution may be viewed as an extension of Pocklington's[15] equation for thin wires. However, as pointed out by Mei[16] the Hallén type equivalent equation may be more convenient to solve. Therefore, in this appendix the Hallén type integral equation is derived.

For convenience the current is required to be zero at the ends of the body of revolution then

$$\int_0^L dz'\ I_t(z')\left(k^2 - \frac{\partial^2}{\partial z \partial z'}\right)K(z,z') = -i\,\frac{4\pi k}{\eta}\,E_z^{inc}\ (0,\phi,z) \tag{A1}$$

Observing that

$$\left(\frac{d^2}{dz^2} + k^2\right)\int_0^z d\xi\ g(\xi)\,\frac{\sin k(z-\xi)}{k} = g(z)$$

for an arbitrary function $g(z)$, (A1) may be written

$$\left(\frac{d^2}{dz^2} + k^2\right)\int_0^L dz'\ I_t(z')\ \Pi(z,z') = -i\,\frac{4\pi k}{\eta}\,E_z^{inc}\ (0,\phi,z) \tag{A2}$$

where

$$\Pi(z,z') = f_1(z') \cos kz + f_2(z') \sin kz + \int_0^z d\xi \left[(k^2 - \frac{\partial}{\partial \xi \partial z'})K(\xi,z')\right] \frac{\sin k(z-\xi)}{k} \quad \text{(A3)}$$

with f_1 and f_2 as arbitrary functions which may be chosen for convenience. Integrating by parts as follows*

$$k^2 \int_0^z d\xi\ K(\xi,z') \frac{\sin k(z-\xi)}{k} = [K(\xi,z') \cos(z-\xi)]\Big|_0^z - \int_0^z d\xi \frac{\partial}{\partial \xi} [K(\xi,z')] \cos k(z-\xi) \quad \text{(A4)}$$

and

$$- \int_0^z d\xi \frac{\partial^2}{\partial \xi \partial z'} K(\xi,z') \frac{\sin k(z-\xi)}{k} = [- \frac{\partial}{\partial z'} K(\xi,z') \frac{\sin k(z-\xi)}{k}]\Big|_0^z - \int_0^z d\xi \frac{\partial}{\partial z'} K(\xi,z') \cos k(z-\xi) \quad \text{(A5)}$$

(A3) becomes

$$\Pi(z,z') = K(z,z') - \int_0^z d\xi [\frac{\partial}{\partial \xi} K(\xi,z') + \frac{\partial}{\partial z'} K(\xi,z')] \cos k(z-\xi) \quad \text{(A6)}$$

*The steps in this derivation are similar to those used by Cambrell and Carson.[17]

provided

$$f_1(z') = K(0,z') \ , \quad f_2(z') = -\frac{1}{k}\frac{\partial}{\partial z'} K(0,z')$$

Solving the indicated differential equation in (A2) yields the desired integral equation for the current distribution

$$\int_0^L dz' I_t(z') \, \Pi(z,z') = C_1 \cos kz + C_2 \sin kz - i\frac{4\pi}{\eta}\int_0^z dz' \, E_z^{inc}(0,\phi,z') \sin k(z-z') \qquad (A7)$$

where $\Pi(z,z')$ is given by (A6). It is noted that (A7) is the extension of the Hallén Integral equation from the thin wire dipole to the dipole of revolution. The corresponding integral equation derived by Hallén[5] is only valid for thin structures.

Table 1: Prolate Spheroid Center Current
$E_o = 1.0$ V/m, $k = 1.0$/m, $\varepsilon = 0.99$

$\frac{kL}{2}$	$I_t(L/2)$	
	Boundary Value Problem Formulation[9]	Integral Equation Formulation
1.212	8.136 + i 14.39	8.126 + i 14.38
1.586	27.37 + i 0.2501	27.35 + i 0.2883
2.020	18.23 - i 10.08	18.22 - i 10.07
2.380	15.19 - i 10.55	15.18 - i 10.53
2.525	14.65 - i 10.60	14.65 - i 10.58
2.828	14.11 + i 10.85	14.12 - i 10.83
3.030	13.99 - i 11.23	14.01 - i 11.20
3.173	13.94 - i 11.64	13.96 - i 11.60
3.232	13.92 - i 11.85	13.94 - i 11.81

TABLE 2: MONOPOLE ADMITTANCE FOR FLAT END CAP

$a/\lambda = 0.0423$, $b/a = 1.187$

h/λ	$Y^*_{measured}$	Y_{TEM}	N
0.12	5.6 + i 26.9 m℧	6.11 + i 27.15 m℧	14
.16	19.8 + i 30.6	20.42 + i 30.30	14
.20	29.8 + i 12.8	30.82 + i 12.29	14
.24	19.6 + i 3.7	20.75 + i 2.04	14
.28	12.9 + i 3.9	13.67 + i 2.03	14
.32	9.5 + i 5.7	9.78 + i 5.16	34
.36	7.6 + i 7.7	7.91 + i 6.92	34
.40	6.6 + i 9.6	6.81 + i 8.58	34
.44	6.0 + i 11.5	6.16 + i 10.21	34
.48	5.7 + i 13.4	5.87 + i 11.94	34
.52	5.9 + i 15.4	5.98 + i 13.91	34
.56	6.8 + i 18.0	6.83 + i 16.33	34
.60	9.3 + i 21.8	9.34 + i 19.18	34
.64	15.4 + i 22.3	15.54 + i 20.98	44
.68	21.7 + i 16.4	22.23 + i 14.78	44
.72	18.7 + i 8.5	19.56 + i 6.54	44

*Measured by S. Holly[12]

TABLE 3: MONOPOLE ADMITTANCE FOR FLAT END CAP

$a/\lambda = 0.1129$; $b/a = 1.220$

h/λ	$Y^{*}_{Measured}$	Y_{TEM}	N
0.12	28.9 + i 41.1 m℧	29.28 + i 40.87 m℧	4
.16	37.0 + i 30.8	35.56 + i 27.14	4
.20	34.0 + i 19.0	32.76 + i 15.02	4
.24	26.4 + i 14.3	25.84 + i 11.73	8
.28	20.9 + i 14.1	20.62 + i 11.65	8
.32	18.6 + i 15.6	17.27 + i 12.69	8
.36	15.7 + i 17.7	14.99 + i 15.99	14
.40	14.5 + i 20.1	13.72 + i 18.12	14
.44	14.2 + i 22.7	13.18 + i 20.32	14
.48	14.3 + i 25.4	13.29 + i 23.97	20
.52	16.2 + i 28.8	14.80 + i 26.60	20
.56	19.5 + i 31.3	18.02 + i 28.68	20
.60	24.7 + i 32.0	23.17 + i 29.11	24
.64	28.5 + i 28.6	27.28 + i 24.81	24
.68	28.5 + i 22.8	27.03 + i 19.13	24
.72	25.0 + i 19.6	23.94 + i 15.85	24

*Measured by S. Holly[12]

TABLE 4: MONOPOLE CURRENT DISTRIBUTIONS FOR FLAT END CAP AND SPHERICAL END CAP. $a/\lambda = 0.007022$, $h/\lambda = 0.25$, $b/a = 3.0$

z/h	Spherical End Cap (N = 74)	Flat End Cap (N = 80)
Driving Point	17.60 - i 7.518 mA	16.47 - i 7.680 mA
0.05	17.56 - i 8.466	16.43 - i 8.636
0.10	17.42 - i 9.084	16.30 - i 9.214
0.15	17.19 - i 9.504	16.09 - i 9.672
0.20	16.87 - i 9.776	15.79 - i 9.944
0.25	16.46 - i 9.926	15.42 - i 10.09
0.30	15.96 - i 9.964	14.96 - i 10.13
0.35	15.38 - i 9.900	14.42 - i 10.07
0.40	14.72 - i 9.738	13.81 - i 9.912
0.45	13.98 - i 9.484	13.13 - i 9.660
0.50	13.16 - i 9.136	12.38 - i 9.316
0.55	12.27 - i 8.700	11.55 - i 8.884
0.60	11.30 - i 8.180	10.67 - i 8.368
0.65	10.27 - i 7.576	9.72 - i 7.768
0.70	9.17 - i 6.890	8.71 - i 7.086
0.75	8.01 - i 6.118	7.64 - i 6.322
0.80	6.78 - i 5.262	6.51 - i 5.476
0.85	5.47 - i 4.318	5.31 - i 4.542
0.90	4.07 - i 3.260	4.03 - i 3.504
0.95	2.49 - i 2.028	2.60 - i 2.296
1.00	0.0 - i 0.0	0.48 - i 0.430

Driving Point Current Measured by Mack[12] for a Spherical End Cap is 17.84 - i 7.50

TABLE 5: MONOPOLE ADMITTANCE FOR SPHERICAL END CAP
$a/\lambda = 0.1129$, $b/a = 1.22$

h/λ	$Y^{*}_{Measured}$	Y_{TEM}	N
0.12	10.8 + i 34.5 mʊ	9.38 + i 32.9 mʊ	4
0.16	21.2 + i 43.3	20.8 + i 38.5	8
0.20	34.3 + i 32.9	32.0 + i 29.4	8
0.24	33.1 + i 19.6	31.1 + i 18.2	8
0.28	27.0 + i 15.1	25.5 + i 14.3	18
0.32	22.3 + i 14.4	20.8 + i 14.3	18
0.36	19.0 + i 15.6	17.6 + i 15.4	18
0.40	16.9 + i 17.3	15.5 + i 17.0	18
0.44	15.8 + i 19.6	14.3 + i 18.9	18
0.48	15.0 + i 22.1	13.7 + i 21.0	18
0.52	15.1 + i 24.9	14.0 + i 23.2	18
0.56	16.6 + i 28.0	15.4 + i 26.4	24
0.60	19.7 + i 30.2	18.4 + i 28.2	24
0.64	24.4 + i 30.3	22.8 + i 27.9	24
0.68	28.3 + i 27.2	26.3 + i 24.1	24
0.72	28.8 + i 22.5	26.1 + i 19.2	24

*Measured by S. Holly[12]

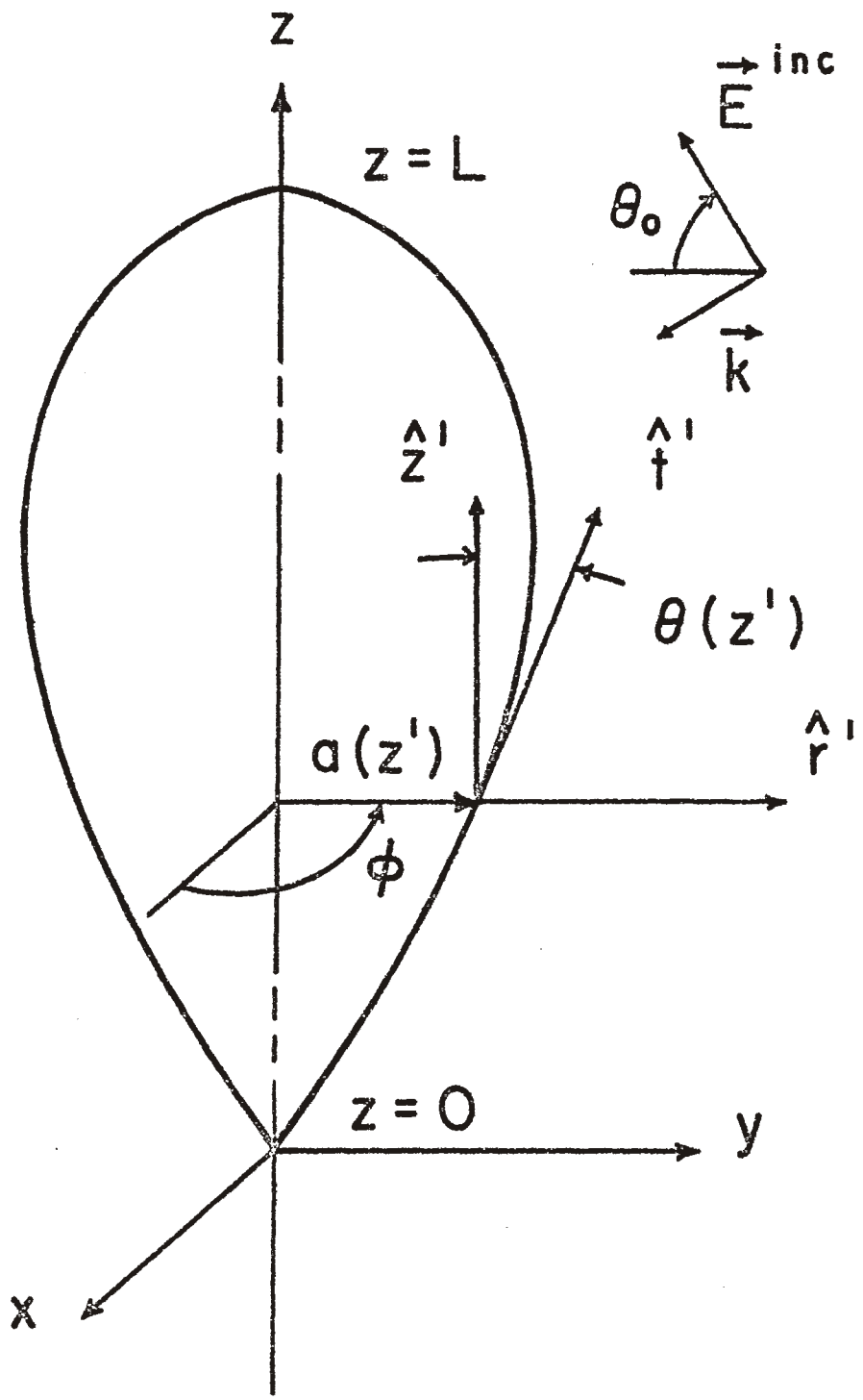

Figure 1: The Body of Revolution with the cylindrical coordinate system.